Numerical Simulation for Dimensioning a Rock Heating Experiment

Author P. Rálek[1], Author M. Hokr[1*]
[1]Technical University of Liberec, Liberec, Czech Republic
*Corresponding author: milan.hokr@tul.cz

Abstract: The paper deals with simulation of rock heating experiment in underground, testing the rock properties for geothermal application. The modeled process is unsteady heat conduction in 3D. We made several parametric studies to find the possible temperature range with uncertainty in some of the parameters - in particular an interval around the laboratory measured heat conductivity and capacity and heat transfer coefficient of the rock surface, including a consideration whether to use an isolation layer on the tunnel face. Line profiles are selected to visualize the rate of temperature drop in various directions to efficiently choose sensor positions in the future experiment.

Keywords: heat transfer, rock heating, geothermal, energy storage.

1. Introduction

The presented work is motivated by preparation of rock heating experiment in underground, for testing the rock properties for geothermal application, energy storage, or spent nuclear fuel disposal [1,2]. The experiment will be placed at the Underground Educational Facility Josef in Central Bohemia (Czech Republic) [3] and adapts the concept of former experiments like [4, 5] to local conditions and particular application.

1.1 Experiment

The experiment is of meter scale, with the heater installed in a large horizontal borehole placed at the tunnel heading. The borehole consists of two parts: the first 2m is filled with isolation material; the remaining 0.5m contains the heater and the geo–polymer filling. There are two possibilities, how to proceed the heater's behavior: either the heater produces constant power in time (e.g. direct electric heating), or we regulate its power in order to have constant temperature (heated water pipe).

According to the experiment concept, the numerical model was designed to estimate the dimensioning of the experiment and describe the effect of using the isolation layer on the tunnel heading.

1.2 Model geometry

In the model, some simplification of the reality was made. We consider, that the tunnel has a strictly symmetrical shape (Fig. 1). The model domain is a cube with 20 long side, without the 10m long part of the tunnel (empty space, Fig. 2). The dimensions are considered to exceed the rock volume influenced by the experiment, which is later confirmed by the simulation results.

All dimensions of the model geometry are parameterized, and can be changed (stated dimensions were used according to the final instructions from the managers of the experiment).

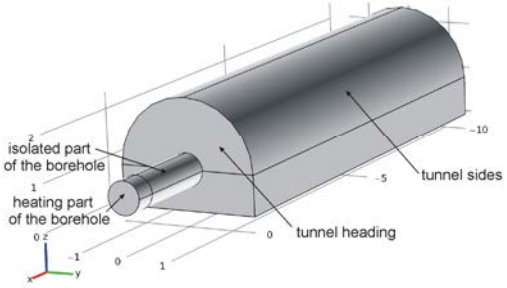

Figure 1. Detail of the tunnel with the borehole.

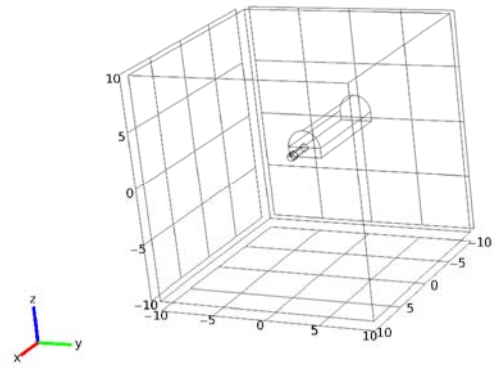

Figure 2. Geometry of the whole modeled domain.

2. Physical description

The modeled process is the unsteady heat conduction in solid. At the boundaries of the tunnel, we suppose the convective cooling. At the boundaries of the whole cubic domain, we suppose to be no influence of the heating process (constant rock temperature).

2.1 Governing equations

The unsteady heat transfer is described by the governing equation

$$\varrho C_P \frac{\partial T}{\partial t} = \nabla \cdot (k \nabla T\ ) + Q$$

where T is the temperature, C_P is the heat capacity under the constant pressure, k is the thermal conductivity, t is the time and Q is the heat source.
Boundary conditions are

$$T = T_0 \quad on\ \partial\Omega_D$$

where Ω_D is the external boundary of the cubic domain. For the tunnel sides, we prescribe the heat transfer

$$\mathbf{n} \cdot (k \nabla T) = h_x (T_1 - T) \quad on\ \partial\Omega_x$$

where Ω_x is a part of the tunnel boundary and h_x is the corresponding heat transfer coefficient (x = "head" for the tunnel heading, x = "sides" for the bottom and sides of the tunnel), **n** is normal vector of the boundary, T_0 is prescribed temperature of the granite massif, T_1 is prescribed air temperature inside the tunnel. We distinguish the heat transfer at the tunnel heading (where an isolation layer can be used) and at the remaining sides of the tunnel (where the heat transfer is influenced only by ventilation).

3. Numerical solution

3.1 COMSOL modules

We used the Heat Transfer module, namely heat transfer in solids (hts) for three different parts of the geometry with different material properties:

- hts in granite massif,
- hts in isolated part of the borehole,
- hts in the heating part of the borehole,

with convective cooling for two parts of the tunnel boundaries:

- convective cooling on the head of the tunnel with heat transfer coefficient h_{head},
- convective cooling on the remaining sides of the tunnel with heat transfer coefficient h_{sides}.

Material properties are used as parameters, and for particular solved tasks (see Table 1) we use Parametric Sweeps.

3.2 Solved tasks

We assume several values for boundary and initial conditions, which remain the same for all solved tasks:

- initial temperature in the whole domain: 283K,
- constant temperature $T_0 = T_1$ on the domain boundaries and inside the tunnel: 283K ,
- heating part of the borehole is simply represented by an iron-like material with the perfect heat conductivity (50000 W/m.K),
- in the centre of the heating part, there is the point heat source with power of 1000W (the power was chosen experimentally such that the maximum temperature reached the desired value 90 °C),
- isolated part of the borehole is represented by the concrete-like material with small heat conductivity (0.9 W/m.K).

We do not know exactly the thermal properties of the really used geo-polymer in the heating part of the borehole, so we use its simplified representation, described above.

The main input uncertainties of the model are the influences of the tunnel ventilation and the heat transfer through the isolation on the tunnel heading. We have solved several tasks for different values of the heat transfer coefficients and also for different values of heat conductivity of granite around the laboratory measured value. The parameters used for four different tasks are listed in the Table 1.

These studies were solved as stationary. Then, for selected material parameters (from task IV with k = 2.6 W/m.K), we solve the time dependent problem with an exponentially increasing time step as the reference case to illustrate the progress of the heating experiment.

Task	h_{head} [W/m^2.K]	h_{sides} [W/m^2.K]	k [W/m.K]
I	0.1	2, 20, 200	2.6
II	0.5	2, 20, 200	2.6
III	2, 20, 200	2, 20, 200	2.6
IV	0.5	20	2.34, 2.6, 2.86

Table 1. Input material parameters for solved tasks.

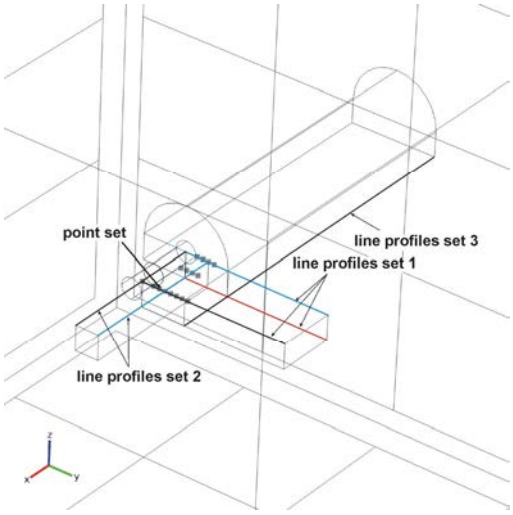

Figure 3. Line profiles and control points used to visualize the results.

4. Results

4.1 Visualization of the results

In the post-processing stage, line profiles (Fig. 3) are presented to analyze the rate of temperature drop in various directions to efficiently choose sensor positions in the future experiment. Colors of the lines on Fig. 3 correspond to the colors used in the graph in the Appendix.

For the visualization of time dependent problem we use the control points set, which represents the way how the real temperature measurement will be executed.

The results are shown in graphs in the Appendix. For tasks I-III, the three subtasks are always plotted together. The line with the maximum temperature belongs to the smallest used heat transfer coefficient; line with the minimum temperature belongs to the largest used heat transfer coefficient.

4.2 Sensitivity of the maximum temperature to the heat conductivity of the rock massif

The maximum temperature depends mainly on the thermal conductivity of the rock massif (Fig. 7, 13) and it is only slightly influenced by the heat transfer at the tunnel heading (isolation layer) or tunnel sides. Decrease of parameter k by value 0.26 W/m.K (Task IV) results in the growth of maximum temperature by value 8°C. Increase of the parameter h_{head} causes the maximum temperature drop by value about 1°C and it is almost uninfluenced by the change of the parameter h_{sides}.

4.3 Influence of the heat transfer to the temperature at the tunnel surface

The influence of the heat transfer to the temperature of the tunnel heading surface is bigger than to the maximum temperature. It is mostly evident from the left bottom part of the graph in Fig. 6 (Task III). Ten times smaller parameter h_{head} (stronger isolation) results in the temperature growth at the surface by about 6-7°C.

The heat transfer also influences the course of the temperature along the tunnel side and its change from the tunnel surface inside the rock massif (Fig. 8, 9, 10). If we do not use the ventilation (the parameter h_{sides} is small), there is visible growth of the temperature (1-2°C) at the tunnel side even in a large distance from the tunnel heading. The isolation of the tunnel heading influences the shape of the temperature course near the tunnel heading. For the small parameter h_{head} (strong isolation), the temperature grows very slowly along the line profile 3, until it reached the tunnel heading; then it starts to grow rapidly. For the large parameter h_{head} (weak isolation), the temperature grows regularly (compare the middle line in Fig. 8, 11, which is for $h_{head} = 0.1$ *and* $h_{sides} = 20$, with the middle line in Fig. 9, 12, which is for $h_{head} = 20$ *and* $h_{sides} = 20$).

The influence of the isolation layer (for $h_{head} = 0.1$) to the shape of the temperature field is displayed in the Fig. 16.

4.4 Time progress of the temperature at the control points

The time progress of the temperature in unsteady heating process is shown in the Fig. 15. The early stage of the heating process, is shown in the Fig. 14, from which the sequential response of the temperature values at the control points (marked in Fig. 3) is visible. While the first response is very quick (few hours), the time to approach the steady state is several months.

5. Conclusion

The results show, that the depth of the borehole and heater shape are well selected – quite low heat loss into the tunnel which is visible from slightly asymmetric temperature contours and moderate sensitivity to the heat transfer (convection).

With the expected uncertainty in parameters (heat conductivity and convective cooling heat transfer) it is possible to plan the experiment to fit the maximum temperature within the 10°C wide interval.

6. References

1. H. Hokmark, B. Falth, Thermal dimensioning of the deep repository. Influence of canister spacing, canister power, rock thermal properties and nearfield design on the maximum canister surface temperature, *SKB report*, **TR-03-09** (2003)
2. H.F Zhang, X.S. Ge, H. Ye, Modeling of a space heating and cooling system with seasonal energy storage, *Energy*, **32**, p. 51–58 (2007)
3. The JOSEF Underground Educational Facility, Czech Technical University, http://www.uef-josef.eu/ (2011)
4. E. Detournay, T. Senjuntichai, I. Berchenko, An in situ thermo–hydraulic experiment in a saturated granite II: analysis and parameter estimation, *Int. J. Rock Mech. Min. Sci.*, **41**, p. 1395–1411 (2004)
5. I. Javandel, P.A. Witherspoon, *Thermal Analysis of the Stripa Heater Test Data From the Full Scale Drift*, 124 pp., Lawrence Berkeley National Laboratory, LBNL-13217, (1981)

7. Acknowledgements

This work was realized under the state subsidy of the Czech Republic within the research project FR-TI3/325 supported by Ministry of Industry and Trade.

8. Appendix – results

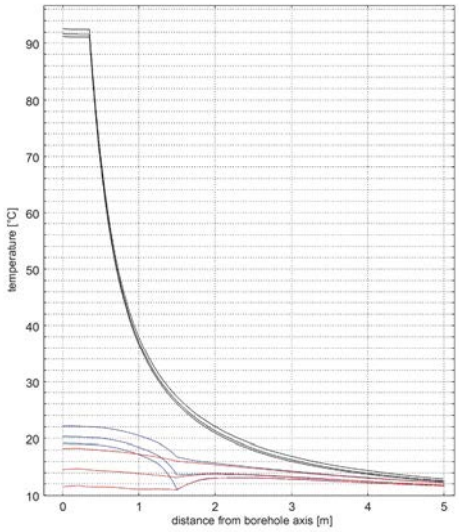

Figure 4. Temperatures in profile set 1, task I.

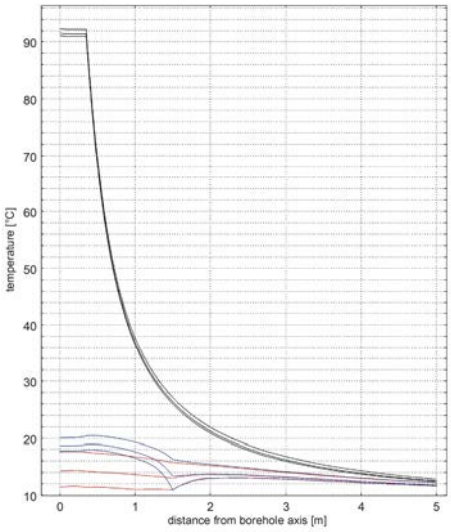

Figure 5. Temperatures in profile set 1, task II.

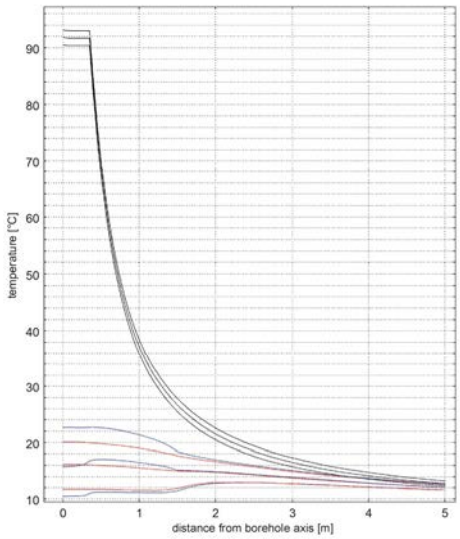

Figure 6. Temperatures in profile set 1, task III.

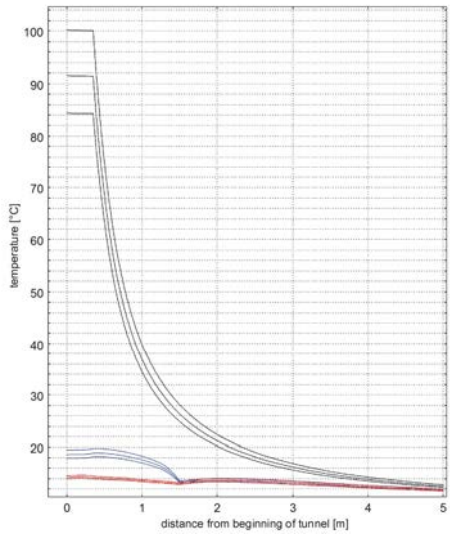

Figure 7. Temperatures in profile set 1, task IV.

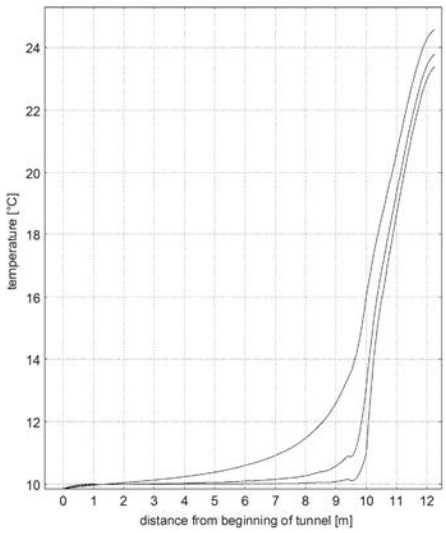

Figure 8. Temperatures in profile set 3, task I.

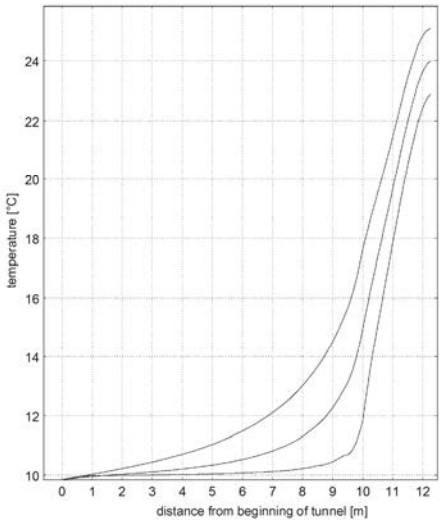

Figure 9. Temperatures in profile set 3, task III.

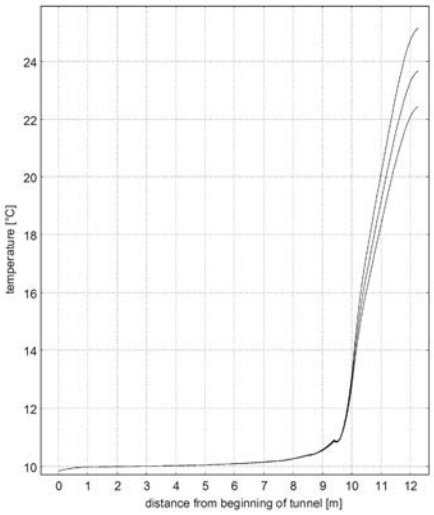

Figure 10. Temperatures in profile set 3, task IV.

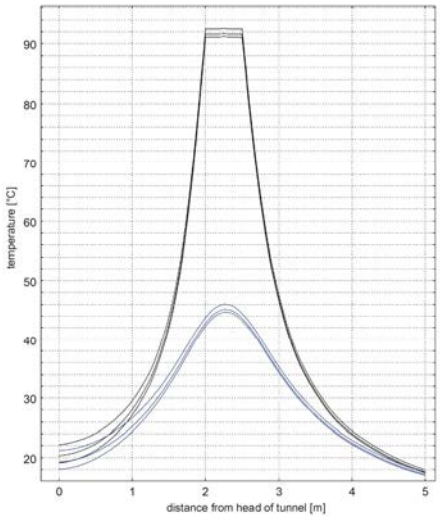

Figure 11. Temperatures in profile set 2, task I.

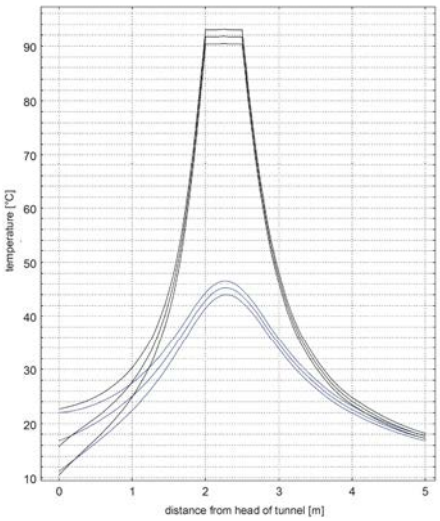

Figure 12. Temperatures in profile set 2, task III.

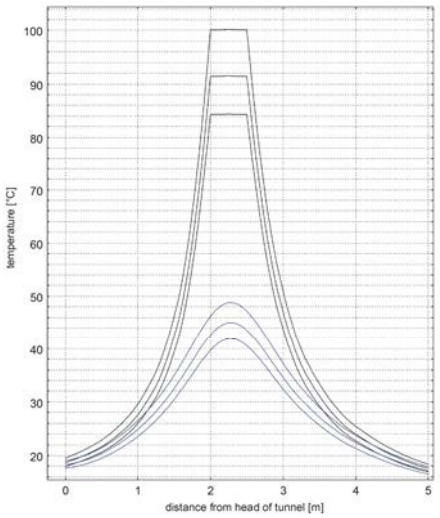

Figure 13. Temperatures in profile set 2, task IV.

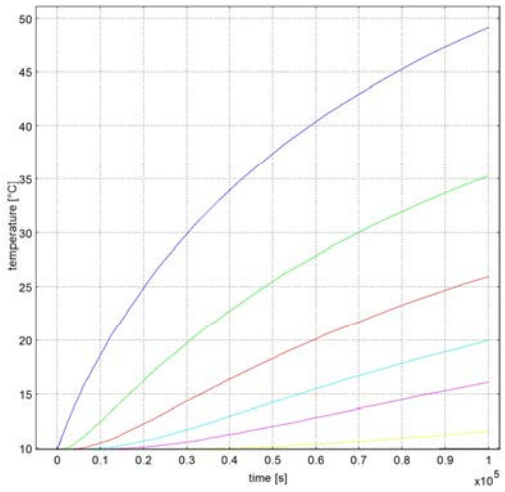

Figure 14. Temperature progress at the control points – early stage (with y-coordinates [m] 0.35, 0.45, 0.55, 0.65, 0.75, 1).

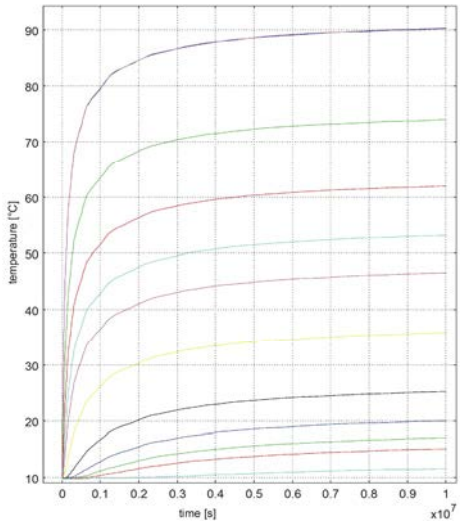

Figure 15. Temperature progress at the control points (with y-coordinates [m] 0.35, 0.45, 0.55, 0.65, 0.75, 1, 1.5, 2, 2.5, 3, 5).

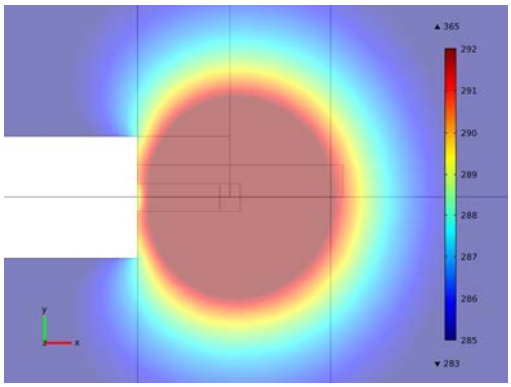

Figure 16. Temperature field, detailed xy-slice through the middle of the heater (temperatures greater then 292K are not distinguished).

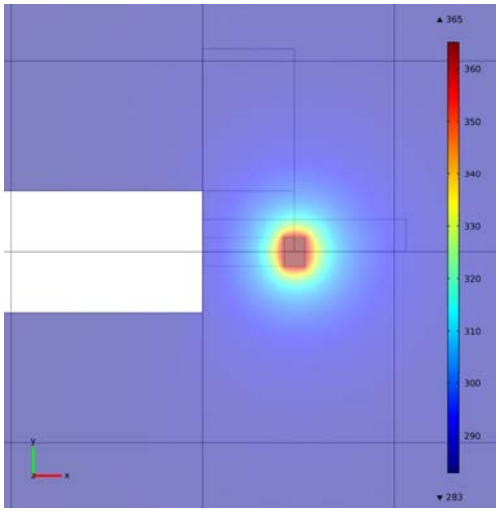

Figure 17. Temperature field, xy-slice through the middle of the heater (Task I, h=20W/m^2.K).

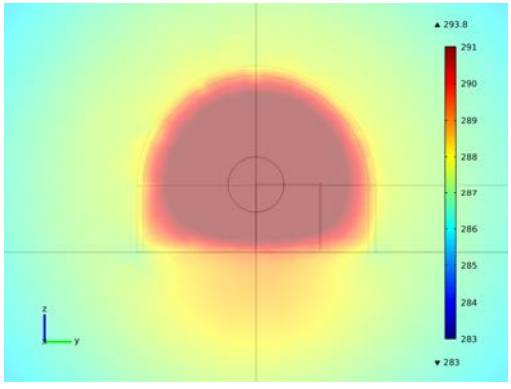

Figure 18. Temperature field, detailed yz-slice near the tunnel heading (temperatures greater then 291K are not distinguished).

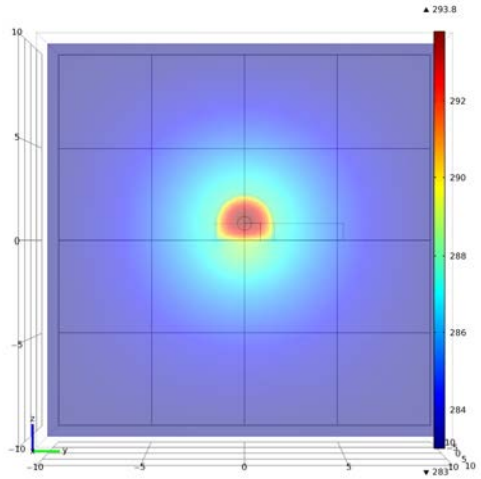

Figure 19. Temperature field, yz-slice near the tunnel heading (Task I, h_{sides} = 20 W/m^2.K).